Journal of Applied Mechanics and Technical Physics, Vol. 49, No. 1, pp. 148–155, 2008

CALCULATION OF THE STRENGTH OF REINFORCED CONCRETE COLUMNS UNDER REPEATED LONGITUDINAL IMPACT

N. N. Belov, N. T. Yugov, D. G. Kopanitsa, O. V. Kabantsev, A. A. Yugov, and A. N. Ovechkina

UDC 539.3

This paper reports the results of experiments with reinforced concrete column models subjected to repeated longitudinal impact loading using a pile driver. The strength of the column models is analyzed by comparing experimental data with results of mathematical modeling.

Key words: *impact, failure, reinforced concrete, mathematical modeling.*

The collapse of concrete-frame buildings under seismic impacts is characterized by failure of the concrete column body with a loss of stability of the longitudinal reinforcement, i.e., buckling of reinforcement bars in various directions, leading to the collapse of the structure or the entire building.

Figure 1 shows the failure of the middle reinforced concrete column of the ground floor of the service center building resulting from the magnitude 7.9 earthquake on October 4, 1994 at the Goryachie Klyuchi village (the Iturup island). One can see the crushed top of the concrete column and the buckling of the main reinforcing bar due to the insufficient transverse reinforcement.

Seismic calculations for concrete frame structures can be based on the results obtained for models of individual members. It should be taken into account that, during seismic impacts, the frame members are subjected to multiple shock loading. In the present work, the failure of models of concrete and reinforced concrete columns under longitudinal impact was analyzed using computational and experimental methods. The experimental studies of repeated shock loading were performed on a pile driver. Mathematical modeling, combined with the laboratory experiments, provided a more complete analysis and valid physical interpretation of test results.

A mathematical model for calculating deformation and failure in porous high-strength ceramics under high-velocity impact and explosion conditions is proposed in [1, 2]. Failure is treated as the formation, growth, and coalescence of microdefects under the action of stresses during loading. The model proposed in [2–4] has been used in failure calculations of brittle materials under multiple shock loading aimed at studying the particle crushing mechanisms in producing submicron-size powders of high-melting compounds in a pneumatic circulating device. In [5], this model was employed to calculate the dynamic strength of concrete.

1. Experimental Studies. Reinforced concrete columns of dimensions $10 \times 10 \times 100$ cm were made of B35 concrete and reinforced by a frame. A-III type longitudinal reinforcement of diameter 10 mm and Bp-I type transverse reinforcement of diameter 5 mm with a step 15 cm were used. The structures were installed vertically on a steel platform. The drop weight acted on the top surface through a steel distributing sheet 2 cm thick. In the experiments, the mass of the drop weight was varied from 225 to 500 kg. The weight drop height was varied from 35 to 70 cm. The measuring system was located inside a steel plate which was placed on the column head and impacted by the weight. The measurements were made by a 32-channel receiving-measuring complex in real time. The time-and-frequency parameters of the columns were determined on a personal computer using the certificated ASTtest program. All stages of the strain state, from elastic strain to failure, were revealed by analyzing the power spectrum and accelerogram fluctuations.

Tomsk State University of Architecture and Building, Tomsk 634003; Yugalex@sibmail.com. Translated from Prikladnaya Mekhanika i Tekhnicheskaya Fizika, Vol. 49, No. 1, pp. 181–190, January–February, 2008. Original article submitted August 1, 2006; revision submitted February 27, 2007.

Fig. 1. Failure of the middle reinforced concrete column of the ground floor of the service center building at the Goryachie Klyuchi village (the Iturup island) as a result of an earthquake of magnitude 7.9.

The first impact of a 225 kg weight dropped from a height of 35 cm did not cause visible damage to the concrete columns. The failure patterns after the second impact are presented in Fig. 2. Failure of two types was observed. In one case, the failure zone formed at the top of the concrete column and was about 1/10 of the height. The longitudinal impact caused symmetric failure of the column head (Fig. 2a). In the other case, the failure region extended to 1/3 of the sample height, leading to spalling of the head (Fig. 2b).

Figure 3 gives failure patterns in a reinforced concrete column after the first and second impacts of a 275 kg weight. The weight dropped from a height of 70 cm. Near the column head, concrete is partly spalled, exposing the longitudinal reinforcement bars. After the second impact, the concrete body of the column head collapsed, resulting in buckling of the longitudinal reinforcement in different directions.

2. Mathematical Modeling. In the calculations, the action of the drop weight on the end surface of the prism was modeled by specifying velocity of the steel plate:

$$u = u_0(1 - t/T).$$

Assuming that, at the steel–concrete interface, the pressure changes with time according to a triangular law, from the second Newton law

$$\frac{m}{S_1}\frac{du}{dt} = P_0\Big(1 - \frac{t}{T}\Big),$$

we determine the time of action of the weight T:

$$T = \frac{2m}{S_1}\frac{V_0}{P_0}.$$

Here m is the mass of the drop weight, S_1 is the cross-sectional area of the prism, $V_0 = \sqrt{2gh}$ is the velocity of the drop weight, and h is the drop height. The pressure P_0 and particle velocity u_0 on the concrete–steel interface can be calculated by a graphic method, using the shock adiabats of steel and concrete [6, 7].

Concrete contains a large number of stress concentrators (pores, grain boundaries, and cracks), on which failure begins in the elastic deformation region. Microfailures can appear in concrete under compression by shear stresses, which leads to a sharp reduction in the resistance to failure.

The nonuniform porous medium is modeled as a two-component material consisting of a solid phase (matrix) and inclusions (pores). It is assumed that the pore shape is almost spherical and that the size distribution function is such that we can introduce the common characteristic size a_0 for the entire ensemble of pores. The specific volume of the porous medium v can be represented as the sum of the specific volume of the matrix material v_m, the specific pore volume v_p, and the specific volume v_c formed during crack opening: $v = v_m + v_p + v_c$. The porosity of the material is characterized by the relative volume of voids $\xi = \xi_p + \xi_c$ or the parameter $\alpha = v/v_m$ ($\xi_p = v_p/v$

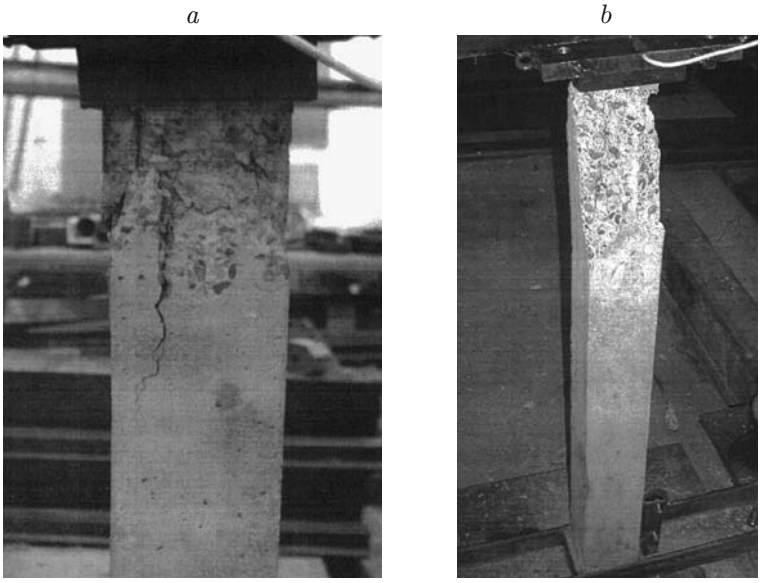

Fig. 2. Failure patterns in concrete columns after the second impact of a 225 kg weight dropped from a height of 35 cm: (a) failure of the first type; (b) failure of the second type.

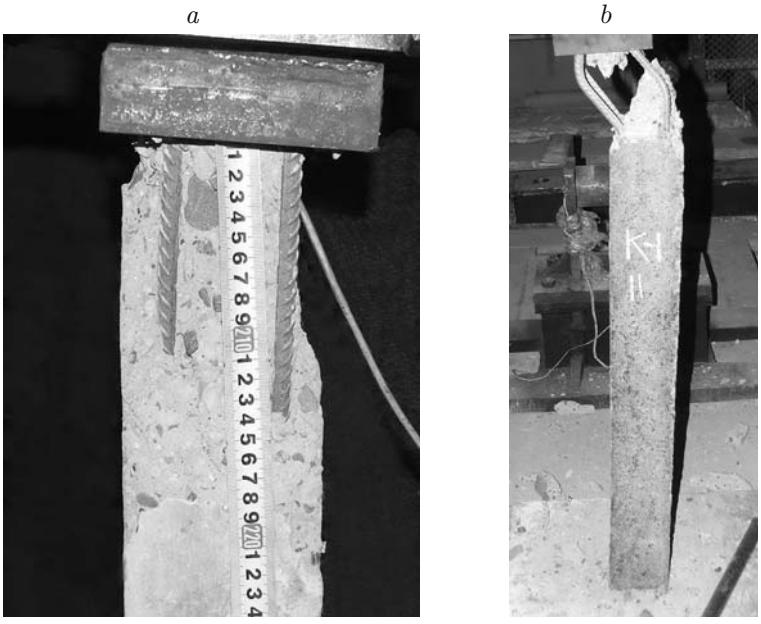

Fig. 3. Failure of a reinforced concrete column after the first (a) and second (b) impacts of a 275 kg weight dropped from a height of 70 cm.

and $\xi_c = v_c/v$ are the relative volumes of the pores and cracks, respectively [2, 5–7]). These parameters are related by the dependence $\alpha = 1/(1-\xi)$.

The system of equations describing the motion of a porous elastoplastic medium is written as

$$\frac{d}{dt}\int\limits_V \rho\,dV = 0, \qquad \frac{d}{dt}\int\limits_V \rho\boldsymbol{u}\,dV = \int\limits_S \boldsymbol{n}\cdot\sigma\,dS, \qquad \frac{d}{dt}\int\limits_V \rho E\,dV = \int\limits_S \boldsymbol{n}\cdot\sigma\cdot\boldsymbol{u}\,dS,$$
$$e = \frac{s^{\mathrm{J}}}{2\mu} + \lambda s, \qquad s:s = \frac{2}{3}\sigma_{\mathrm{t}}^2, \qquad p = \frac{\rho_0}{\alpha}\Big(\gamma_0\varepsilon + \frac{c_0^2(1-\gamma_0\eta/2)\eta}{(1-S_0\eta)^2}\Big), \tag{2.1}$$

where t is time, V is the domain of integration, S is the boundary of the domain of integration, $\boldsymbol{n}$ is the unit vector of the outward normal, ρ is the density, $\sigma = -pg + s$ is the stress tensor, s is the stress deviator, p is the pressure, g is the metric tensor, $\boldsymbol{u}$ is the velocity vector, $E = \varepsilon + \boldsymbol{u}\cdot\boldsymbol{u}/2$ is the specific total energy, ε is the specific internal energy, $e = d - (d:g)g/3$ is the strain rate deviator, $d = (\nabla\boldsymbol{u} + \nabla\boldsymbol{u}^{\mathrm{t}})/2$ is the strain rate tensor, $s^{\mathrm{J}} = \dot{s} + s\cdot\omega - \omega\cdot s$ is the derivative of the stress deviator in the Jaumann–Noll sense, $\mu = \mu_0(1-\xi)[1 - (6\rho_0 c_0^2 + 12\mu_0)\xi/(9\rho_0 c_0^2 + 8\mu_0)]$ is the shear modulus, $\sigma_{\mathrm{t}} = \{\sigma_{\min} + (\sigma_{\max} - \sigma_{\min})kp/[(\sigma_{\max} - \sigma_{\min}) + kp]\}/\alpha$ is the yield limit, $\omega = (\nabla\boldsymbol{u}^{\mathrm{t}} - \nabla\boldsymbol{u})/2$ is the vortex tensor, ρ_0, c_0, μ_0, $\sigma_{\min}$, $\sigma_{\max}$, k, S_0, and γ_0 are constants of the matrix material, and $\eta = 1 - \rho_0 v/\alpha$. The parameter λ is eliminated by means of the yield condition.

To close system (2.1), we need the equations describing the variation of the parameter α in tension and compression. Failure of brittle materials is due mainly to the occurrence and growth of microcracks. The maximum elastic half-opening of a coin-shaped crack under the action of a tensile stress perpendicular to the plane of the crack is given by the relation

$$\delta = -2(1-\nu)Rp_m/(\pi\mu_0),$$

where ν is Poisson's ratio, R is the crack radius, and $p_m = \alpha p$ is the pressure in the matrix material. Assuming that the opening crack faces form an ellipsoid of revolution with the semiaxes δ, R, and R, we find the volume of the crack

$$V_c = -8(1-\nu)R^3\alpha p/(3\mu_0). \tag{2.2}$$

Let no new cracks be formed during loading and let the deformation of the material be accompanied by growth of the initially existing cracks of the characteristic size R. Then, relation (2.2) implies that

$$\xi_c = -8(1-\nu)N_0R^3\alpha p/(3\mu_0) \tag{2.3}$$

(N_0 is the number of cracks in unit volume). Taking into account that, before the beginning of fragmentation of the cracked material, the pore volume remains constant and equal to ξ_0, we have

$$\xi_c = \xi - \xi_0 = (\alpha - \alpha_0)/(\alpha_0\alpha). \tag{2.4}$$

Substituting (2.4) into (2.3), we finally obtain

$$p = -\frac{3\mu_0(\alpha - \alpha_0)}{8(1-\nu)N_0\alpha_0R^3\alpha^2}. \tag{2.5}$$

From Eq. (2.5) it follows that as the crack radius increases, the growth of discontinuities becomes faster. The rate of increase in the crack size is given by the equation

$$\dot{R}/R = F_1 + F_2,$$

where $F_1 = (\alpha s_i - s_*)/\eta_1$ at $\alpha s_i > s_*$, $F_1 = 0$ at $\alpha s_i \leqslant s_*$, $F_2 = (|\alpha p| - p_*)/\eta_2$ at $p < 0 \wedge |\alpha p| > p_*$, $F_2 = 0$ at $p \geqslant 0 \vee |\alpha p| \leqslant p_*$, $s_i = \sqrt{(3/2)s:s}$, $s_* = s_{01}(1 - R/R_*)$, $p_* = (1 - R/R_*)$, $R_* = \beta/\sqrt[3]{N_0}$, and s_{01}, η_1, η_2, and β are constants of the material.

From the third equation in (2.1) and (2.5), we obtain the following equation for the parameter α for elastic deformation of concrete:

$$\Big(\gamma_0\varepsilon\rho_0 + \frac{\rho_0 c_0^2(1-\gamma_0\eta/2)\eta}{(1-S_0\eta)^2}\Big) + \frac{3\mu_0(\alpha - \alpha_0)}{8(1-\nu)N_0\alpha_0R^3\alpha^2} = 0.$$

In the case of plastic materials, coalescence of microcracks occurs by their direct contact. Calculations of a system of elastic cracks have shown that their interaction and coalescence occur at a distance between their

nearest crack tips of the order of two or three crack sizes [8]. This critical distance depends on the size of the zone around the crack in which the stress concentration is significant. Constructing a quantitative model for microdefect coalescence, including the formation of microscopic fragments, is a difficult problem. It is assumed that coalescence of microcracks begins when their characteristic size R, with a constant number of cracks in unit volume N_0, reaches the critical value $R_* = \beta/\sqrt[3]{N_0}$. The fragmentation of the cracked material and the behavior of the fractured material are described by the model of a porous elastoplastic medium. System (2.1) is closed by the equations relating the pressure p and porosity α:

— for compression $[p \geqslant (2/3)\sigma_{\rm t} \ln(\alpha/(\alpha-1))]$,

$$\gamma_0 \varepsilon \rho_0 + \frac{\rho_0 c_0^2 (1-\gamma_0\eta/2)\eta}{(1-S_0\eta)^2} - \frac{2}{3}\,\sigma_{\rm t} \ln\Big(\frac{\alpha}{\alpha-1}\Big) = 0;$$

— for unloading $[p \leqslant -a_s \ln(\alpha/(\alpha-1))]$,

$$\gamma_0 \varepsilon \rho_0 + \frac{\rho_0 c_0^2 (1-\gamma_0\eta/2)\eta}{(1-S_0\eta)^2} + a_s \ln\Big(\frac{\alpha}{\alpha-1}\Big) = 0.$$

The fragmentation of the cracked material subjected to tensile stresses occurs when the relative volume of voids reaches the critical value $\xi_* = (\alpha_* - 1)/\alpha_*$. If the cracked material is subjected to compressive stresses, the fragmentation criterion is the ultimate plastic strain intensity

$$e_u = (\sqrt{2}/3)\sqrt{3T_2 - T_1^2}$$

(T_1 and T_2 are the first and second invariants of the strain tensor, respectively). The fragmented material in tension is described as a powder which moves according to the equations of a stress-free material [9, 10].

Calculations of the strength of reinforced concrete columns under impact and shock loading involves difficulties of computational nature. A comparison of the actual column dimensions with the diameters of the reinforcing bars shows that, in considering the real reinforcement, one needs to choose small steps in both space and integration time. To reduce the computation volume, we change the computation scheme as follows: the reinforcing bar with adjoining concrete is replaced by an elastoplastic medium, which is a homogeneous two-phase mixture of steel and concrete, whose initial density $\rho_{0\text{r.c.}}$ is given by the formula

$$\rho_{0\text{r.c.}} = \nu_1 \rho_{0\text{s}} + \nu_2 \rho_{\text{c}}.$$

Here ν_1, ν_2, $\rho_{0\text{s}}$, and $\rho_{0\text{c}}$ are the initial volume concentrations and densities of steel and concrete ($\nu_1 + \nu_2 = 1$). Thus, a cylindrical steel bar of diameter d is replaced by a tetrahedral prism from the specified mixture of cross-sectional area S_2.

The volume concentrations are determined through the areas occupied by steel and concrete in a section perpendicular to the direction of the bar:

$$\nu_1 = \pi d^2/(4S_2), \qquad \nu_2 = 1 - \nu_1.$$

The equation of state for the reinforced concrete (mixture) is written as

$$p_m = \frac{\rho_{0\text{r.c.}} c_{0\text{mix}}^2 (1-\gamma_{\text{mix}}\eta/2)}{(1-S_{0\text{mix}}\eta)^2} + \gamma_{\text{mix}} \rho_{0\text{r.c.}} \varepsilon,$$

where $\eta = 1 - \rho_{0\text{r.c.}} v$ (v is the specific volume of the mixture), γ_{mix} is the Grüneisen coefficient, and $v_{0\text{r.c.}} = 1/\rho_{0\text{r.c.}}$.

The coefficients $c_{0\text{mix}}$ and $S_{0\text{mix}}$ of the linear dependence $D = c_{0\text{mix}} + S_{0\text{mix}} u$ (dependence of the shock-wave velocity D in the mixture on the particle velocity u) are determined in terms of the shock adiabats of the mixture components:

$$D_i = c_{0i} + S_{0i} u_i \qquad (i = 1, 2).$$

In the variables v_m and p_m, the equation of the shock adiabat of the mixture is written as

$$v_m(p_m) = \sum_{i=1}^{2} \Big\{ v_{0i} - \frac{1}{p_m} \Big[\frac{c_{0i}}{S_{0i}} \Big(\sqrt{\frac{S_{0i} p_m}{\rho_{0i} c_{0i}^2} + \frac{1}{4}} - \frac{1}{2} \Big) \Big]^2 \Big\} m_i.$$

Using the shock-wave relations for the mixture

$$D = v_{0\text{r.c.}} \sqrt{p_m/(v_{0\text{r.c.}} - v_m(p_m))}, \qquad u = \sqrt{p_m (v_{0\text{r.c.}} - v_m(p_m))},$$

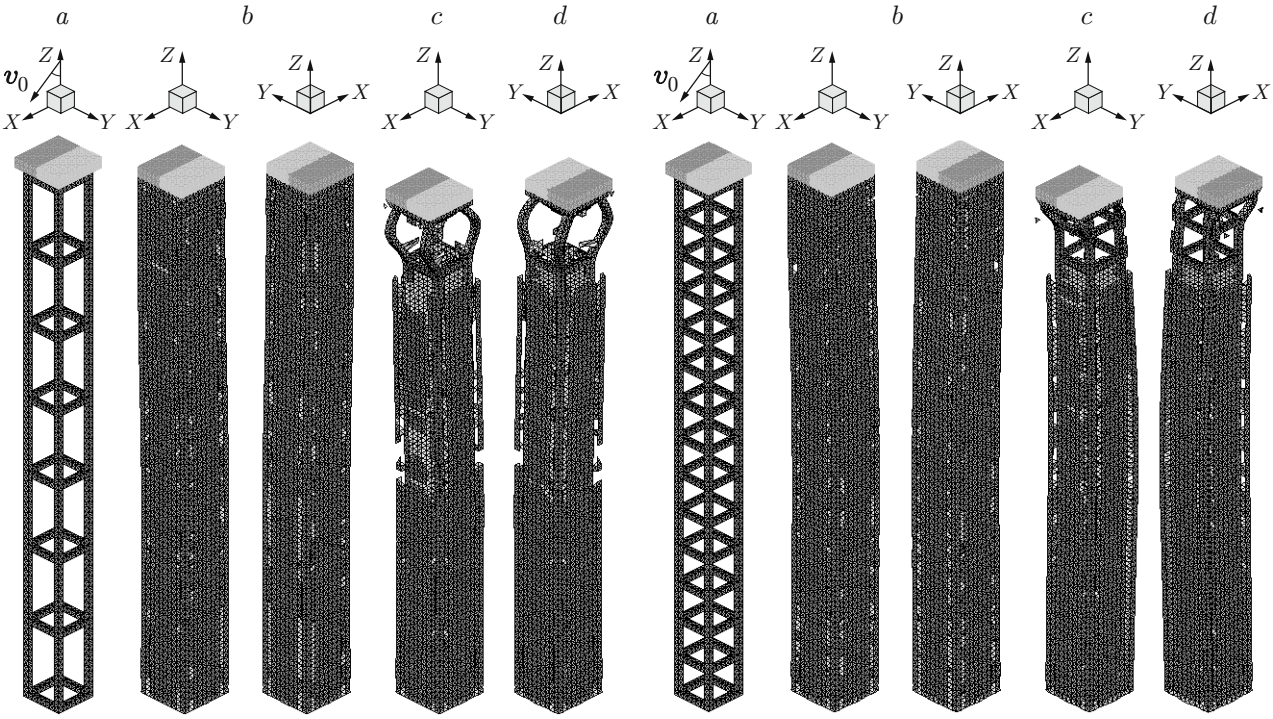

Fig. 4

Fig. 5

Fig. 4. Configurations of the reinforcement and column after the first and second impacts at $l =$ 15 cm: configuration of the reinforcement frame (a), reinforced column (b), and failure modes after the first impact (c) and after the second impact (d).

Fig. 5. Configurations of the reinforcement and column after the first and second impacts at $l = 8$ cm (notation the same as in Fig. 4).

we can construct the dependence of the shock-wave velocity on the particle velocity and determine the coefficients $c_{0\mathrm{mix}}$ and $S_{0\mathrm{mix}}$.

The Grüneisen coefficient γ_{mix} for the mixture is determined in terms of the Grüneisen coefficients of the components γ_{0i}:

$$\frac{v_{0\mathrm{r.c.}}}{\gamma_{\mathrm{mix}}} = \sum_{i=1}^{2} \frac{m_i v_{0i}}{\gamma_{0i}}.$$

The shear modulus of the mixture $\mu_{0\mathrm{mix}}$ and the yield stress $\sigma_{\mathrm{t\,mix}}$ are determined from the formulas

$$\mu_{0\mathrm{mix}} = 1/(\nu_1/\mu_{01} + \nu_2/\mu_{02}), \qquad \sigma_{\mathrm{t\,mix}} = m_1\sigma_{\mathrm{t},1} + m_2\sigma_{\mathrm{t},2},$$

where $m_i = \nu_i\rho_{0i}/\rho_{0\mathrm{r.c.}}$ are the mass concentrations of steel ($i = 1$) and concrete ($i = 2$) in the reinforced concrete layer; μ_{0i} and $\sigma_{\mathrm{t},i}$ ($i = 1, 2$) are the shear moduli and yield stresses of the mixture components, respectively.

3. Calculation Results. The model described above was used to calculate the strength of models of reinforced concrete columns subjected to longitudinal repeated impact by a 275 kg weight dropped from a height of 70 cm.

In the mathematical modeling, two versions of reinforcement were considered to reveal the effect of the arrangement of the transverse reinforcement on the failure of the reinforced concrete columns under repeated shock loading. In the first version, the distance l between the transverse bars was 15 cm, and in the second version, it was 8 cm.

The configurations of the reinforcement frame for both calculation versions are given in Figs. 4 and 5. The longitudinal reinforcing bars were modeled by an elastoplastic mixture of steel and concrete with volume

TABLE 1

Material	ρ_0, g/cm^3	μ_0, GPa	c_0, cm/μsec	γ_0	S_0	$\sigma_{\min}$, GPa	α_0	a_s, GPa	ξ_*	e_u^*
Concrete	2.20	17.00	0.233	2	1.51	0.0077	1.0100	0.042	0.013	0.15
Steel	7.85	82.00	0.457	2	1.49	0.6000	1.0006	0.290	0.300	1.00
Mixture with										
$\nu_1 = 0.200$	3.33	2.10	0.258	2	1.50	0.1300	1.0037	0.086	0.060	0.20
$\nu_1 = 0.330$	4.08	2.52	0.278	2	1.49	0.2100	1.0025	0.150	0.198	0.33
$\nu_1 = 0.785$	6.64	7.35	0.350	2	1.50	0.2600	1.0010	0.170	0.236	0.78

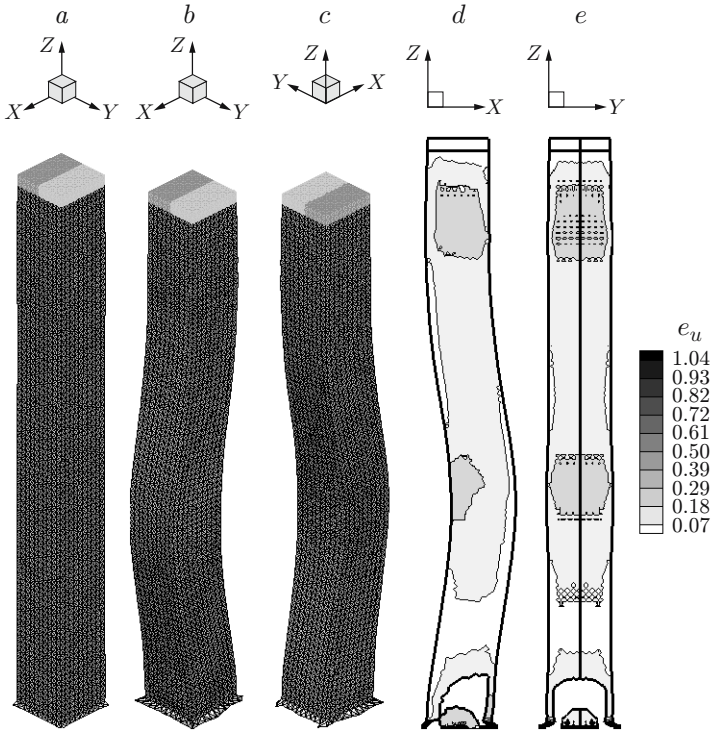

Fig. 6. Results of mathematical modeling of the impact on a concrete column enclosed in a steel shell 3 mm thick: reinforced column (a), configuration of the column after the first impact (b) and after the second impact (c), and plastic strain intensity isolines after the second impact in the planes ZX (d) and ZY (e).

concentrations $\nu_1 = 0.785$ and $\nu_2 = 0.215$, respectively, and transverse reinforcing bars by a similar mixture with volume concentrations $\nu_1 = 0.2$ and $\nu_2 = 0.8$, respectively. This replacement allowed us to model a frame from steel bars in which the longitudinal bars were 1 cm in diameter and transverse bars 0.5 cm. Table 1 gives values of the mechanical parameters of concrete, steel, and their mixtures. In addition, the following mechanical characteristics for concrete were used in the failure models: $\sigma_{\max} = 0.216$ GPa, $k = 0.82$, $\nu = 0.256$, $R_0 = 2.5$ μm, $R_* = 11.6$ μm, $N_0 = 64 \cdot 10^7$ cm^{-3}, $\eta_1 = 7000$ GPa$\cdot$ μsec, $\eta_2 = 800$ GPa$\cdot$ μsec, $p_0 = 0.00924$ GPa, $S_{01} = 0.0924$ GPa, and $\beta = 1$.

The calculation results are presented in Figs. 4 and 5. The slope of the weight velocity to the longitudinal axis of the column is taken from experiment and equals 24°. The initial impact velocity was 3.3 m/sec. For the first impact, the loading time was 12 msec, and for the second impact, it was 24 msec. The increase in the loading time for the repeated impact is due to the fact that the spalling of part of concrete at the column head results in a decrease in the contact area S_1. In the calculation, the first impact did not lead to failure at the head. For a correct comparison of the calculated and experimental results for the repeated impact, the contact surface area S_1 was taken from the experiment.

In both calculation versions, the first impact results in spalling of concrete from the side surfaces and separation of small fragments from the edges. After the repeated impact, as in the experiment, the concrete body

in the head part fails to approximately the same depth. However, a more close arrangement of the transverse reinforcing bars in the second version prevents buckling of the longitudinal reinforcing bars, i.e., at a step of transverse reinforcement $l = 8$ cm, buckling of the reinforcing bars does not occur. In addition to buckling, the bars bend in the direction of the impact.

The results of the mathematical modeling are in good qualitative agreement with the experimental data. The difference is due to the fact that the calculations were performed for an isotropic material, whereas concrete, as a rule, is an anisotropic material. In addition, the shock-wave deformation of a material is influenced by the replacement of cylindrical reinforcing bars with prismatic bars.

Figure 6 gives the results of mathematical modeling of the shock interaction between a 275 kg weight dropped from a height of 70 cm and a concrete column enclosed in a steel shell 3 mm thick. The first impact of duration 12 msec did not lead to failure of the column. The strength calculation for the column after the repeated impact (the first and second impacts are coaxial) was performed for shock loading times of 12 and 24 msec. The degree of failure of the concrete body of the column can be judged by the plastic strain intensity isolines e_u in the planes ZX and ZY (Fig. 6). In the calculations, it was assumed that the fragmentation of the cracked concrete occurred if the plastic strain intensity reached the ultimate value equal to 0.15. In the lower parts of the column, there was rupture of the steel shell. The concrete body of the column is almost entirely cracked ($e_u = 0.07$), but concrete fragmentation is observed only in three regions. The largest region of fragmented material is near the top end ($e_u > 0.15$). The second region of failed material adjoins the shell rupture surface near the bottom end. In this region, primarily cleavage failure and partly shear failure are observed. The third region of fragmented material is near the center of the column. In the vicinity of the top end of the column and in the central region of bending of the column, the fragmentation of cracked concrete occurs by a shear mechanism.

A combination of experimental studies and mathematical modeling provides a more complete analysis and a more correct physical interpretation of experimental data, which is very important in designing buildings in seismic hazard areas.

REFERENCES

1. S. A. Afanas'eva, N. N. Belov, V. F. Tolkachev, et al., "Features of shock-wave deformation of porous Al_2O_3 ceramics," *Dokl. Ross. Akad. Nauk*, **368**, No. 4, 477–479 (1999).
2. N. N. Belov, N. T. Yugov, D. G. Kopanitsa, and A. A. Yugov, *Impact Dynamics and Corresponding Physical Phenomena* [in Russian], STT, Tomsk (2005).
3. N. N. Belov, A. Yu. Biryukov, N. T. Yugov, et al., "Shock interaction of particles of ceramic materials in a pneumatic circulating device," *Vestn. Tomsk. Gos. Arkh.-Stroit. Univ.*, No. 2, 112–128 (2003).
4. N. N. Belov, A. Yu. Biryukov, A. T. Roslyak, et al., "Particle crushing mechanism in producing submicron-size powders of high-melting compounds in a pneumatic circulating device," *Dokl. Ross. Akad. Nauk*, **397**, No. 3, 337–341 (2004).
5. N. N. Belov, N. T. Yugov, D. G. Kopanitsa, and A. A. Yugov, "Model for dynamic failure of fine-grained concrete," *Vestn. Tomsk. Gos. Arkh.- Stroit. Univ.*, No. 1, 14–22 (2005).
6. Ya. B. Zel'dovich and Yu. P. Raizer, *Physics of Shock Waves and High-Temperature Hydrodynamic Phenomena*, Academic Press, New York (1967).
7. N. N. Belov, D. G. Kopanitsa, O. K. Kumpyak, and N. T. Yugov, *Calculation of Reinforced Concrete Structures under Impact and Shock Loading* [in Russian] STT, Tomsk (2004).
8. R. L. Salganik, "Mechanics of solids with a large number of cracks," *Izv. Akad. Nauk SSSR, Mekh. Tverd. Tela*, No. 4, 149–158 (1973).
9. N. N. Belov, N. T. Yugov, D. G. Kopanitsa, and A. A. Yugov, "Strength analysis of concrete and reinforced-concrete slab structures under a high-velocity impact," *J. Appl. Mech. Tech. Phys.*, **46**, No. 3, 444–451 (2005).
10. S. A. Afanas'eva, N. N. Belov, D. G. Kopanitsa, et al., "Failure of concrete and reinforced concrete slabs under a high-velocity impact and shock," *Dokl. Ross. Akad. Nauk*, **401**, No. 2, 185–188 (2005).